

Assessment of soil liquefaction potential using the standard penetration test at Port Sudan

Dafalla Wadi ^{1*} , Husam Eldin Ahmed ² , Ibrahim Malik ³ , Wenbing Wu ⁴ ,
Abuzar Fuad ⁵ 

¹Department of Hydrogeology and Engineering Geology, College of Petroleum Geology and Minerals, University of Bahri, Khartoum, Sudan.

²Sea Ports Corporation, Engineering Tests Lab, Port Sudan, Sudan.

³Department of Geology, Faculty of Petroleum and Minerals, Al-Neelain University, Khartoum, Sudan.

⁴Engineering Research Centre of Rock - Soil Drilling Excavation and Protection, Ministry of Education, China University of Geosciences, Wuhan, Hubei 430074, China.

⁵Department of Chemistry and Earth Science, College of Arts & Sciences, Qatar University, Doha

*Corresponding author email: wadiadam@cug.edu.cn

Received: 09-05-2025 | Accepted: 12-06-2025 | Available online: 15-06-2025 | DOI:10.26629/uzjest.2025.10

ABSTRACT

Liquefaction is one of the most critical ground deformations in saturated or partially saturated silty and sandy soils. This deformation may cause severe destruction, such as settlement and building tilting. A standard penetration test (SPT) is commonly used to estimate liquefaction potential. This study integrates SPT, unit weight, and fine content data measurements from 24 boreholes in Port Sudan to evaluate and identify the liquefaction potential and factor of safety (F.S.) in earthquake scenarios. The liquefaction parameters were derived according to the simplified procedure in this scope. The result showed that the subsurface soil up to 15 meters is saturated with grain sizes varying from medium to fine sand, silt, and clay. Based on calculated parameters and fine content, the area falls within the high risk of liquefaction by a 7.5 (Mw) earthquake. The F.S. is mainly less than one in the upper 15 m. The liquefaction potential index is assessed using a peak horizontal ground acceleration of 0.15 g for an earthquake scenario of magnitude 7.5. The proposed approach proved to be a rapid and reliable method for investigating the liquefaction of sandy soil under earthquakes.

Keywords: Liquefaction, Standard Penetration Test, Liquefaction Potential Index, Factor of safety, Port Sudan

تقييم إمكانية تسهيل التربة باستخدام اختبار الاختراق القياسي في بورتسودان

دفع الله وادي¹، حسام الدين احمد²، إبراهيم مالك³، وينبينغ وو⁴، أبوذر فؤاد⁵

¹ قسم جيولوجيا المياه والجيولوجيا الهندسية، كلية جيولوجيا البترول والمعادن، جامعة بحري، ص.ب. 2469، الخرطوم، السودان.

² مؤسسة الموانئ البحرية، مختبر الاختبارات الهندسية، بورتسودان، السودان.

³ قسم الجيولوجيا، كلية النفط والمعادن، جامعة النيلين، الخرطوم - السودان.

⁴ مركز أبحاث هندسة الصخور وحفر التربة وحمايتها، وزارة التعليم، جامعة الصين للعلوم الجيولوجية، وهان، هوبي 430074، الصين.

⁵ قسم الكيمياء وعلوم الأرض، كلية الآداب والعلوم، جامعة قطر، الدوحة

ملخص البحث

التسييل هو أحد أكثر التشوهات الأرضية أهمية في التربة الطينية والرملية المشبعة أو المشبعة جزئياً. قد يتسبب هذا التشوه في تدمير شديد، مثل الاستقرار وإمالة المباني. يُستخدم اختبار الاختراق القياسي (SPT) بشكل شائع لتقدير إمكانية التسييل. تدمج هذه الدراسة قياسات بيانات اختبار الاختراق القياسي ووزن الوحدة ومحتوى المواد الدقيقة من 24 بئراً في بورتسودان لتقييم وتحديد إمكانية التسييل ومعامل الأمان (F.S.) في سيناريوهات الزلازل. تم اشتقاق معاملات التسييل وفقاً للإجراء المبسط في هذا النطاق. أظهرت النتيجة أن التربة تحت السطحية حتى 15 متراً مشبعة بأحجام حبيبات تتراوح من الرمل المتوسط إلى الناعم والطيني والطين. بناءً على المعلمات المحسوبة والمحتوى الدقيق، تقع المنطقة ضمن خطر التسييل العالي بسبب زلزال بقوة 7.5 (Mw). يكون F.S. أقل من واحد بشكل أساسي في الـ 15 متراً العليا. يُقِيم مؤشر احتمالية التميع باستخدام ذروة تسارع أفقي للأرض مقدارها 0.15 جي لسيناريو زلزال بقوة 7.5 درجة. وقد أثبت النهج المقترح أنه طريقة سريعة وموثوقة لدراسة تمييع التربة الرملية تحت تأثير الزلازل.

الكلمات الدالة: التسييل، اختبار الاختراق القياسي، مؤشر إمكانية التسييل، عامل الأمان، بورتسودان

1. Introduction

The phenomenon of soil liquefaction can be defined as the reduction in shear strength brought on by increased pore pressure in the soil particles due to ground shaking during earthquakes [1]. SPT, or simplified techniques, were created by [1] and are frequently used to evaluate soil liquefaction potential. The SPT technique has been improved and updated since its original proposal by [2–5]. As a result of its simplicity and low cost, SPT is widely used in in-situ tests for soil investigation in engineering schemes [6]. Also, SPT values display the underground density and are used in many geotechnical formulations [7].

Moreover, SPT has some uncertainties due to Equipment and Operator Variability, Energy Efficiency, Soil Disturbance, Borehole Conditions, Sampler Type and Condition, Soil Type Sensitivity, Depth and Overburden Stress, and Empirical Nature. However, the experiment has been widely used to determine soil properties and foundation designs. Furthermore, a study by [8] classified the soil layers based on SPT values. The classification given in Table 1 has been used to define meaningful class borders in the resulting models.

Table 1. Description of standard penetration test (SPT) values [8]

A descriptive term for soil	Very loose	Loose	Medium dense	Dense	Very dense
SPT value	0–4	4–10	10–30	30–50	>50

Classifying fine-grained soils using conventional methods, such as the Chinese criteria, is necessary to assess their susceptibility to liquefaction [9, 10]. In [3], they described the Chinese standard's specific applications. According to their understanding, liquefaction is only possible in the following three conditions: (1) the proportion of particles smaller than 5 m is less than 15%; (2) the liquid limit (L.L.) is less than 35%; and (3) the moisture content (WC) is greater than 0.9 LL. Only a small percentage of recovered soil specimens are categorised as "Susceptible" based on Chinese standards, according to [10]. However, regarding liquefaction, most soil materials are classified as "Not Susceptible or Safe".

During earthquakes, the sand tends to compact during shaking, and water in the pores cannot move away quickly enough, at least in the fine sands, to accommodate the compaction instantaneously. Therefore, stresses are thrown into the water, increasing the pore water pressure and reducing the effective or intergranular stress between the sand particles [11]. Sand particles depend on the effective stress between

their grains to settle, shear strength, and resistance to displacement. Therefore, the increase in pore water pressure leads to strength loss. In some cases, where pore water pressure equals total stress, the sand loses its shear strength entirely and behaves like a viscous fluid [5, 12].

Port Sudan is one of the most important cities in Sudan, lying on the coastal plain of the Red Sea on the country's eastern border (Figure 1). Rapid building construction in the city, together with the increase in the population, has led to the demand for establishing a geological engineering model upon which urban planners, developers, and engineers can rely.

The main aim of this study is to evaluate the liquefaction potential for the Khor Mojj deposit based on SPT data and laboratory tests of the soil samples, focusing on unit weight and fine content properties. The safety factor and liquefaction potential will be identified based on these properties.

This study used the SPT data according to the procedure in [13]. Since the cyclic resistance ratio (CRR) values are lower than the cyclic stress ratio (CSR), the factor of safety (F.S.) is generally below unity. Based on these results, the upper 15 m of subsurface soil will be liquefied by any amount of earthquake with a magnitude equal to or greater than 7.5.

1.1 Geological Setting Of The Study Area

The study area's geological setting lies within the Nubian-Arab Shield, which consists of Precambrian basement rocks outcropping on the flanks of the Red Sea. These crystalline rocks are predominantly Neoproterozoic in age and include metamorphic, metasedimentary, igneous, and sedimentary rocks [14]. Superficial deposits and recent sediments occupy the floodplains and peneplains [15] Figure 1.

Khor Mojj is one of the most significant watercourses, draining from the hilly district in the west and passing through Port Sudan city to the Red Sea in the east (Figure 1). The stream covers a large area with its floodplain. The sediments of this plain consist of saturated, very loose to loose fine sand and silty sand with depths varying from 20 to 30 m. The existing water table is between 0.9 m and 1.9m.

One of the world's most important dynamic rift systems, the Red Sea Rift System, is where Port Sudan City is situated tectonically [16–18]. A variety of rifting phases are included in the rifting. These phases progress through multiple stages of continental rifting, beginning with early faulting [17, 19, 20–23]. The Red Sea is known for its frequent felt earthquakes, which range in magnitude from 3.0 to 6.8 (Figure 2). Onshore, these earthquakes don't present a serious risk. The Red Sea's seismicity suggests that specific Cenozoic faults within the coastal plain are seismically active and should be considered when evaluating seismic risks [24].

2. Materials and Methods

The study area covers 18000 m² with unique topography and is raised a meter above sea level. A total of 24 boreholes were drilled to various depths ranging from 20 to 30 m using the rotary drilling technique. The distribution of the boreholes is shown in Figure 3. Standard Penetration Test (SPT) was conducted at an interval of 1.5 meters, and soil samples were taken with this interval for all drilled boreholes (384 samples were obtained). The sampling procedure (Table 2) consisted of driving a standard split spoo as outlined in [25, 26], and SPT N-values have been normalized according to [25].

The step is repeated blows of the hammer of 63.5kg weight falling through 0.76 m height. Hence, the energy transmitted to the sampler would be assumed to be 60% if no short-rod correction was applied. The remaining 40% is lost due to mechanical inefficiencies and energy dissipation. The main causes are friction Loss, hammer rebound and misalignment, rope stretch and slack, rod joint and thread Loss, soil and borehole conditions, and hammer type and drop system.

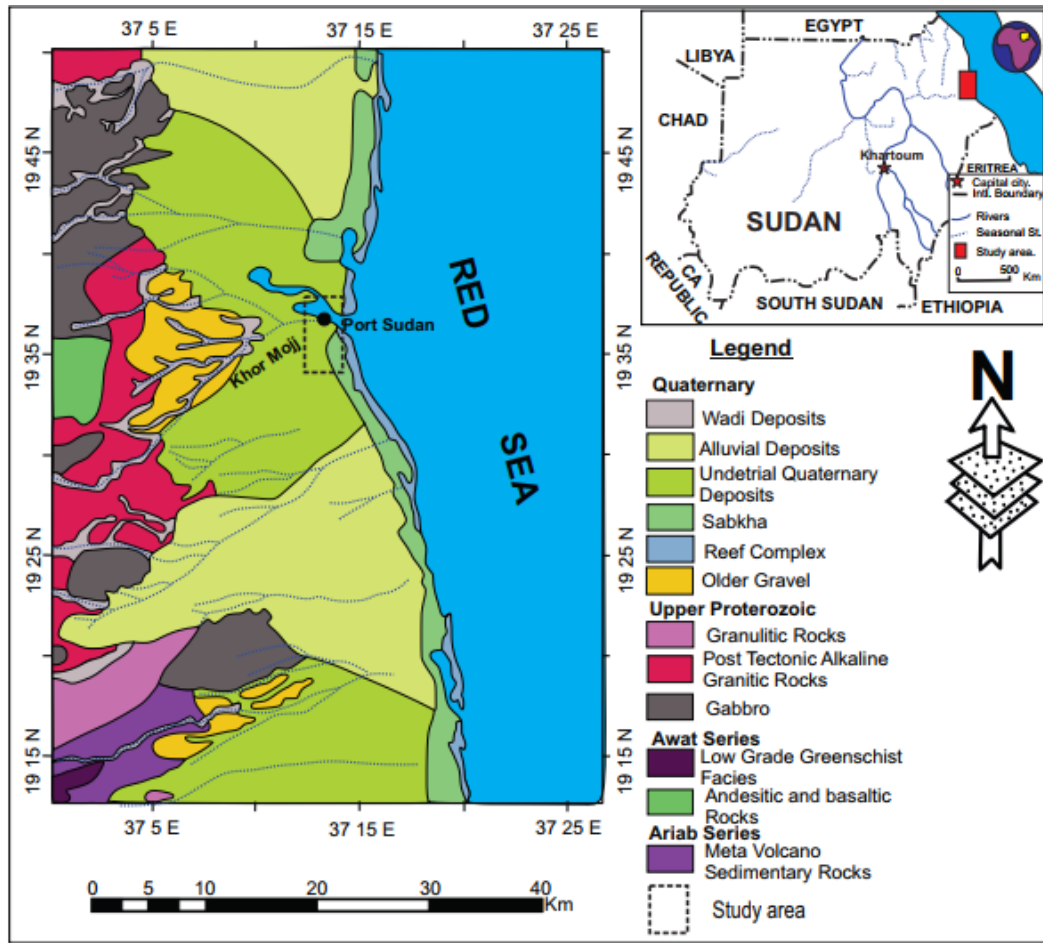


Figure 1. Geological map of the study area (modified after [15])

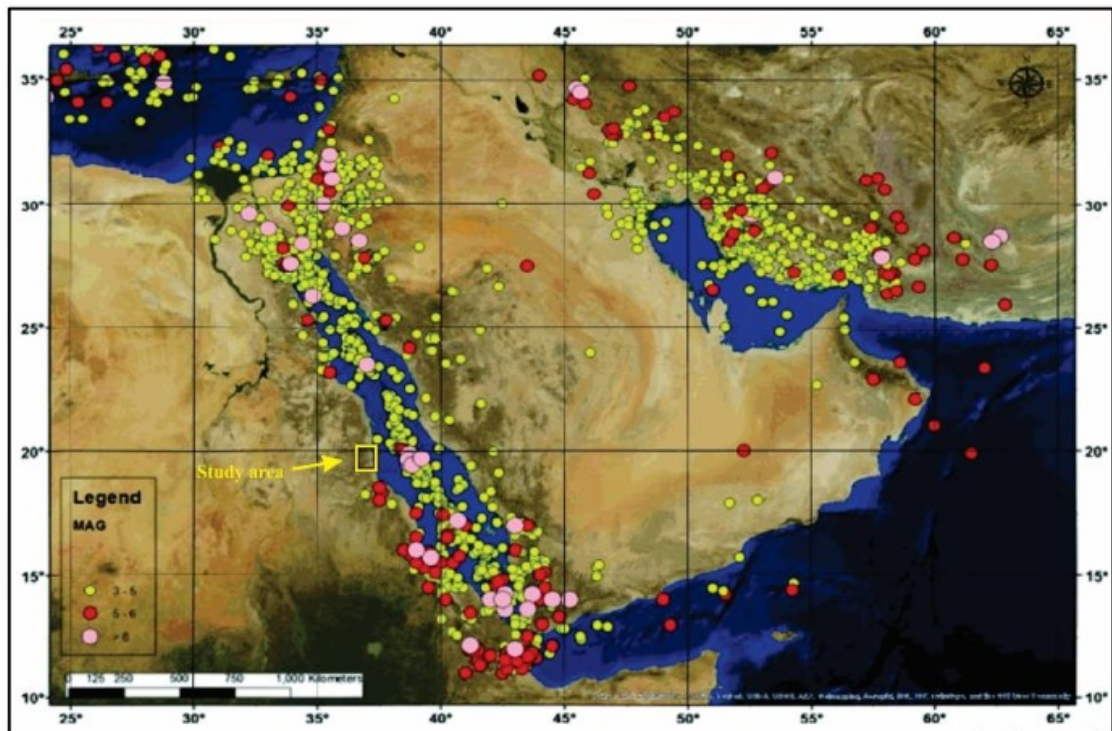


Figure 2. Seismicity up to 2013, including historical and instrumental earthquakes above MI 3.

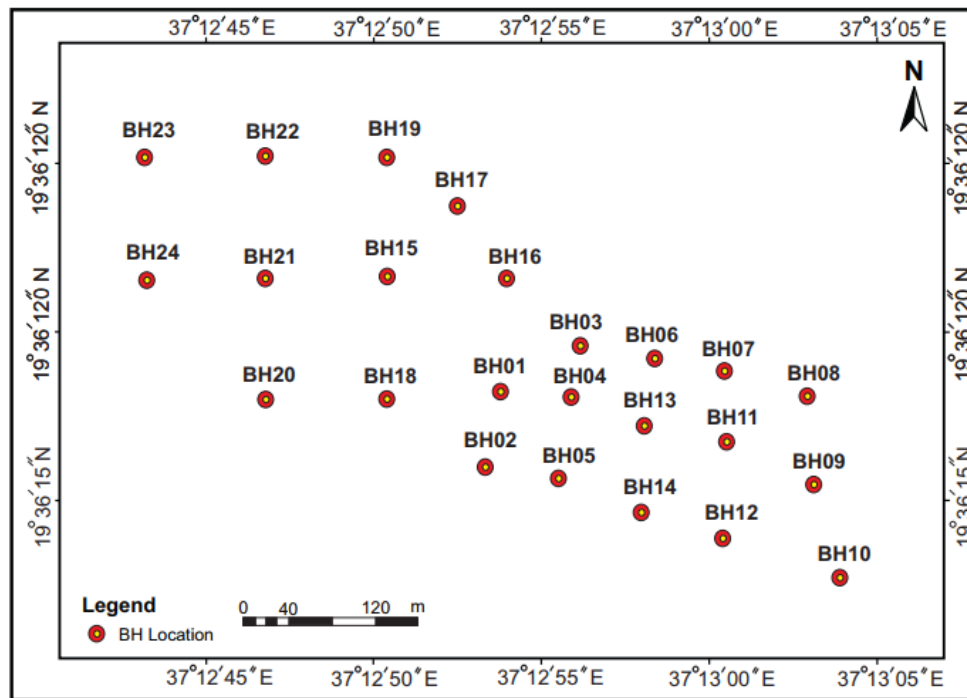


Figure 3. Location map of test boreholes

In each borehole, samples were taken every 1.5 meters. A split spoon sampler was used to gather disturbed samples. For disrupted samples, we used a split spoon sampler; for undisturbed samples, we used a U-tube sampler. To enhance and bolster the findings of in-situ studies, laboratory tests are performed on both disturbed and undisturbed samples taken from the boreholes. The tests are conducted in accordance with British Standard BS 1377 and include Atterberg limits, unit weight, and grain size analysis.

Table 2. Procedure Used for the Standard Penetration Test

Drilling methods	Rotary with bentonite mud
Drill bit	Tri-cone bit (9 cm diameter)
Drill rod	Area = 5.94 cm ² , length = 1.52 m
Sampler	Outer diameter = 50.8 mm, inner diameter = 35 mm, length = 600 mm.
Cathead and rope	2 $\frac{1}{4}$ turns of rope (2 cm diameter) on a clockwise rotating cathead (11.2 cm diameter)
Hammer type	Safety hammer
Penetration resistance	Blows were recorded over three intervals, each 15 cm; N = blows over the last two intervals.

2.1 Liquefaction Evaluation Framework

To determine the soil factor of safety and liquefaction, in-situ testing and laboratory findings have been combined in accordance with the methodology in [13]. The input parameters are SPT data, fine content, median diameter, influence depth, and friction angle. Every borehole is subjected to the measurement. The total liquefaction potential was assessed in accordance with [27].

Normalizing the measured N-values by any hammer is essential to a standard rod energy ratio. The standard conversion $N_{60} = N (E_{rr}/60)$ can normalize the measured N-values with a known or estimated rod energy ratio (ERr) value. Skempton pointed out in [28] that the blow count in a given soil is inversely proportional to the rod energy ratio (ERr). Unlike hammer kinds and release systems, he also provided

the rod energy ratio. Based on that, the ERr ratio is 60%, and the ERr/60 ratio equals 1.0. Therefore, N60 equals the measured N-value, which can be used directly in the Analysis.

The study in [27] proposed the stress-based liquefaction potential determination approach, which has been extensively used for the last five decades [1 – 3], [11], [29 – 31]. The fundamental idea behind this method is the relationship between the soil's cyclic resistance ratios (CRRs) and the cyclic stress ratios (CSRs) caused by earthquakes. This context's components were developed to offer a logical approach to the many variables influencing penetration and cycle resistance.

According to [11], the following expression can be used to determine the earthquake-induced CSR at a specific depth inside the soil profile:

$$CSR_{m,\sigma'_v} = 0.65 \frac{\tau_{max}}{\sigma'_v}. \quad (1)$$

Where τ_{max} is the maximum earthquake-induced shear stress; σ'_v is effective vertical stress.

The maximum shear stress can also be calculated through the simplified procedure developed by [1]:

$$CSR_{m,\sigma'_v} = 0.65 \frac{\sigma_v}{\sigma'_v} \frac{\alpha_{max}}{g} r_d. \quad (2)$$

Where σ_v is total vertical stress at depth z , $\frac{\alpha_{max}}{g}$ is the maximum horizontal acceleration at the ground surface, and r_d is shear stress reduction factor that accounts for the dynamic response of the soil profile.

The study presented by [11] pointed out that CRR of the soil is generally connected to an in-situ test, such as SPT blow count, cone penetration test (CPT), or shear wave velocity, Vs. The correlation to CRR is based on corrected penetration resistance, which can be expressed as:

$$(N_1)_{60} = C_N C_E C_R C_B C_S N_M. \quad (3)$$

where the overburden correction factor is denoted by C_N . $C_E = ERm/60\%$, where ERm is the average energy expressed as a percentage of the hammer energy of free fall. N_M is the measured SPT blow count; C_R is the rod correction factor to account for smaller energy ratios with shorter rod lengths; C_B is the correction factor for nonstandard borehole diameters; C_S is a correction factor for using split spoons with space for liners but without them; and C_T is the rod correction factor for nonstandard borehole diameters. When conventional processes are followed, the elements C_B and C_S equal unity.

The fine components of soil (F.C.) impact the connection between CRR and $(N_1)_{60}$. By [11], this effect can be expressed mathematically in terms of an equivalent clean-sand $(N_1)_{60cs}$, which can be found using the following formula:

$$(N_1)_{60cs} = (N_1)_{60} + \Delta(N_1)_{60}. \quad (4)$$

Then CRR can be written as:

$$CRR_{m=7.5,\sigma'_v=1atm} = f[(N_1)_{60cs}]. \quad (5)$$

According to [32], the safety factor against liquefaction (F.S.) of a soil layer can be estimated using many approaches, such as SPT and CPT, which are unsuitable for assessing the severity of liquefaction, although they can predict its occurrence. They stressed that F.S. is not a valuable parameter in making liquefaction severity maps for liquefaction-prone areas. It can be used to predict layer liquefaction, but not degrees of severity. A study by [27] has proposed a potential liquefaction index (LPI) to overcome the limitation of F.S. These researchers suggested that damage to the structures tends to be severe if the liquefiable layer is thick and shallow. The Factor of Safety (F.S.) for the liquefiable layer is significantly less than 1.0. The following formulas state the original form of the LPI:

$$LPI = \int_0^{20} F(z)W(z)dz. \quad (6)$$

$$F(z) = 1 - FS \text{ for } FS < 1.0. \quad (7)$$

$$F(z) = 0 - FS \text{ for } FS \geq 1.0. \quad (8)$$

$$W(z) = 10 - 0.5z \text{ for } z < 20m. \quad (9)$$

$$W(z) = 0 \text{ for } z > 20m. \quad (10)$$

Where z is the depth to the mid-point of the layer in meters.

Table 3 represents the liquefaction severity categories proposed by [33] in an updated form. The table was initially developed by [27].

Table 3. Liquefaction potential classification proposed by [33]

LPI	Liquefaction potential category
0	Non-liquefiable (based on $FS \geq 1.2$)
$0 < LPI \leq 2$	Low
$2 < LPI \leq 5$	Moderate
$5 < LPI \leq 15$	High
$15 > LPI$	Very high

3. Results and Discussion

3.1 Results

This study evaluates liquefaction potential based on grain-size distribution, lithological borehole logs, standard penetration-test blow count (SPT-N), and unit weight of soils data set. Liquefaction potential has been evaluated for all boreholes in the study area. The depth varies from 25 to 30 meters. From grain size and lithology logs, we notice clear stratification of the soil in all boreholes (Figure 4); this generally consists of different lithologies such as silty sand, fine silt, clayey sand, and sandy clay, although soil lithology is composed of the same grain size with different colors, plasticity index, and stiffness.

SPT-N values in the study area generally range from 0 to 20, indicating loose to medium-dense soils. An exception is borehole 9, where the SPT-N reached a maximum of 24 between 16.5 m and 26.5 m. Figure 5a indicates that the CRR curve for percent fines $\geq 35\%$ derived from SPT applies to most SPT-based liquefaction triggering analyses. Atterberg Limits test of fine soil shows liquid limit values ranging between 17% and 61% and plasticity indices in the 1% to 29% range.

Most of the Cyclic Stress Ratio values of soil layers of boreholes under investigation (CSR red curve in Figure 5a) have values greater than 0.2 at shallow depth and decrease with depth, reaching less than 0.05, which indicates an increase in soil stiffness with depth. On the other hand, the Cyclic Resistance Ratio (CRR black curve) also significantly increases with depth, starting from 0.086 at shallow depth and 0.2 at deeper depth. However, some anomalies are shown on wells 5 and 15; the values reached 1.0.

Using a maximal horizontal ground acceleration of 0.15g and the earthquake scenario with $M_w=7.5$, the liquefaction potential index (LPI) was calculated for each drilled borehole in the research region. When the analysis was conducted, the water table was still at 1.4 meters. Its readings progressively drop with depth, going from 10.11 (high potential) at 1.5 m to 0 (non-liquefiable) at about 15 m. (Table 4 and Figure 6).

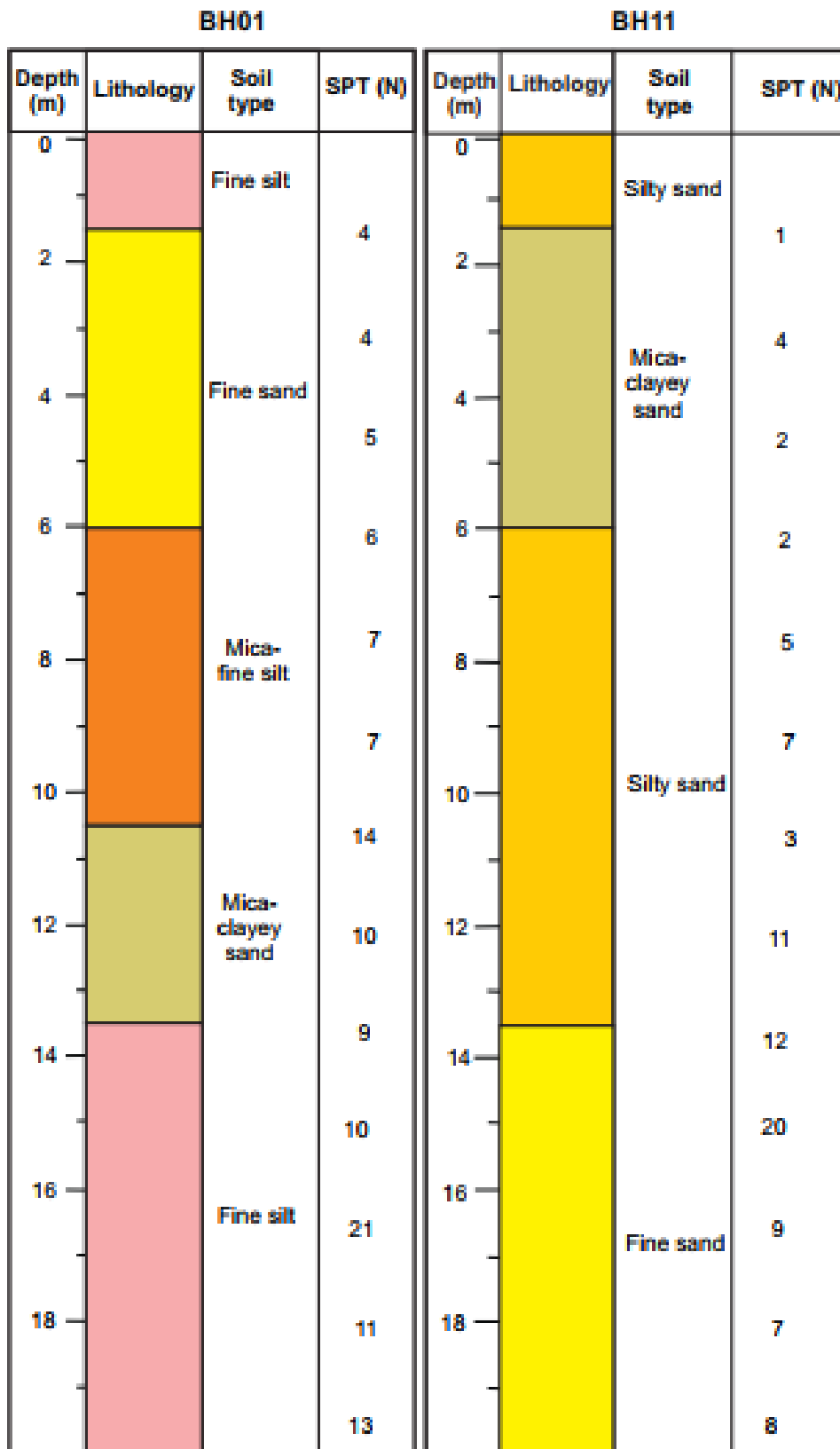


Figure 4. Two examples of the SPT data logs are representative of the study area

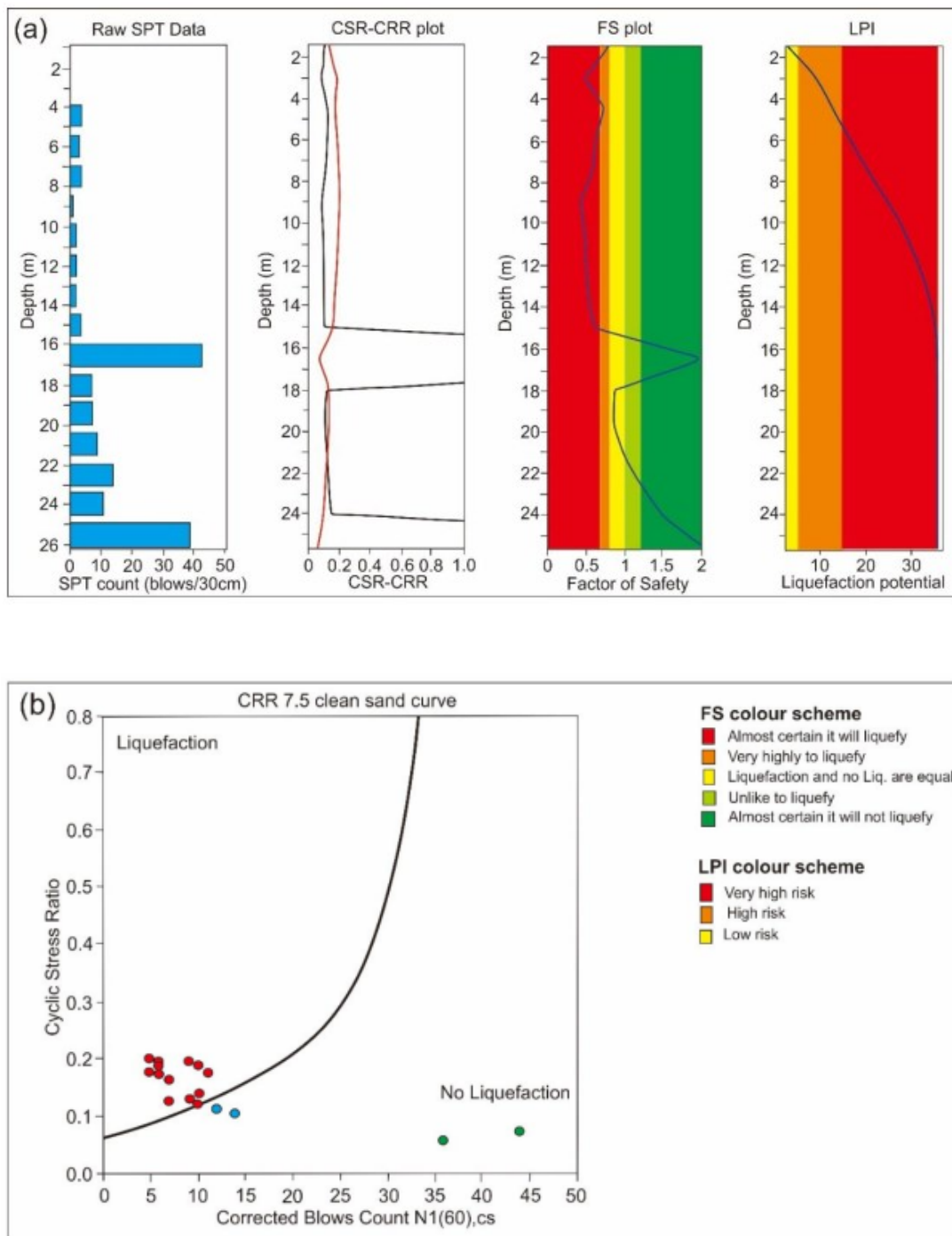


Figure 5. shows an example of the SPT data logs representative for the study area, using a peak horizontal ground acceleration of 0.15 g for a magnitude 7.5 (Mw) earthquake: (a) raw data, CSR-CRR plot, F.S. plot, and LPI; (b) cross-plot of CRS against corrected blow count.

The factor of safety (F.S.) increases with depth, as indicated in the graphs, starting from 0.25 at a shallow depth to 2.0 at greater depths. However, a high anomaly has been noticed at depths of 15 to 18 meters for all boreholes, indicating the presence of a stiff layer (Figure 5a).

Cross plot of CRS against corrected blow count ($N_{1(60),cs}$) were used to indicate the samples' vulnerability to liquefaction. The results suggest that most samples lie in the liquefaction zone (Figure 5b).

Table 4. An example of a variation of soil properties with depth

Depth (m)	(N ₁) _{60CS}	Fine content (%)	Unit weight (KN/m ³)	CSR	CRR _{7.5}	FS	LPI
1.5	7	64	16.14	0.125	0.098	0.788	6.48
3.0	5	16	17.33	0.175	0.086	0.492	3.23
4.5	11	59	16.00	0.173	0.125	0.722	3.87
6.0	10	59	16.00	0.187	0.118	0.631	3.93
7.5	9	18	17.16	0.191	0.111	0.581	4.72
9.0	5	19	17.26	0.201	0.086	0.428	3.7
10.5	6	20	17.30	0.191	0.092	0.481	2.97
12.0	6	16	17.32	0.183	0.092	0.504	2.28
13.5	6	17	17.46	0.173	0.092	0.523	1.46
15.0	7	14	17.54	0.161	0.098	0.610	0.00
16.5	44	18	17.54	0.07	4	2.000	0.19
18.0	10	18	17.36	0.135	0.118	0.872	0.06
19.5	9	19	17.60	0.131	0.111	0.852	0.00
21.0	10	13	17.56	0.121	0.118	0.974	0.00
22.5	12	12	17.73	0.11	0.132	1.203	0.00
24.0	14	69	16.19	0.101	0.148	1.471	0.00
25.5	36	33	17.34	0.057	4	2.000	0.00

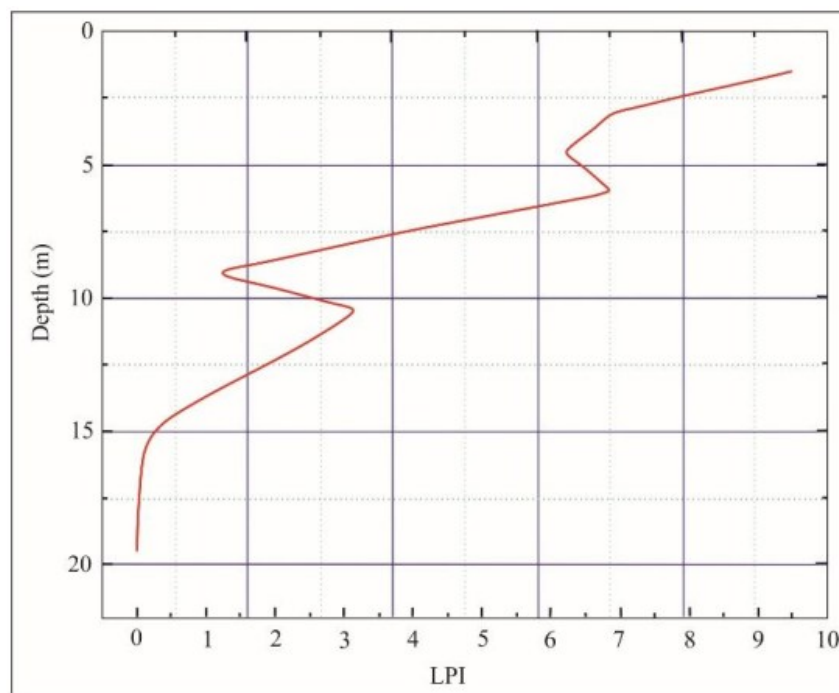


Figure 6. LPI measured at borehole 13 of the study area, using a peak horizontal ground acceleration of 0.15 g for a magnitude 7.5 (M_w) earthquake, where the water table remains to a depth of 1.4 m

3.1.1 Results interpolation

SPT can be used to get information about a particular topic. It is expensive and time-consuming to measure every area [34]. For a trustworthy evaluation, the information regarding the unsampled sites must be accessible. Interpolation should be used to estimate the unsampled

places to get around this issue. Many interpolation techniques may frequently forecast the unsampled areas with acceptable errors, even though many are presented [7]. Because they employ a stochastic approach, geostatistical methods like Gaussian simulation, sequential indicator simulation, and simulated annealing are powerful instruments for estimating, interpolating, and forecasting unsampled points. Building the variogram and Kriging model can accomplish these methods [35, 36].

The simulation algorithms consider both the variety of estimations at unsampled places and the spatial variation of real data at sampled locations [37]. The stochastic simulation respects the sample data in their original places and replicates the sample statistics (variogram and histogram model) [7]. To characterise the subsurface soil in the districts of Khor Mojj, this study employed sequential indicator simulation (SIS). Figs. 7–10 present the interpolation of borehole logs, SPT values, a factor of safety, and liquefaction potential, respectively.

3.2 Discussion

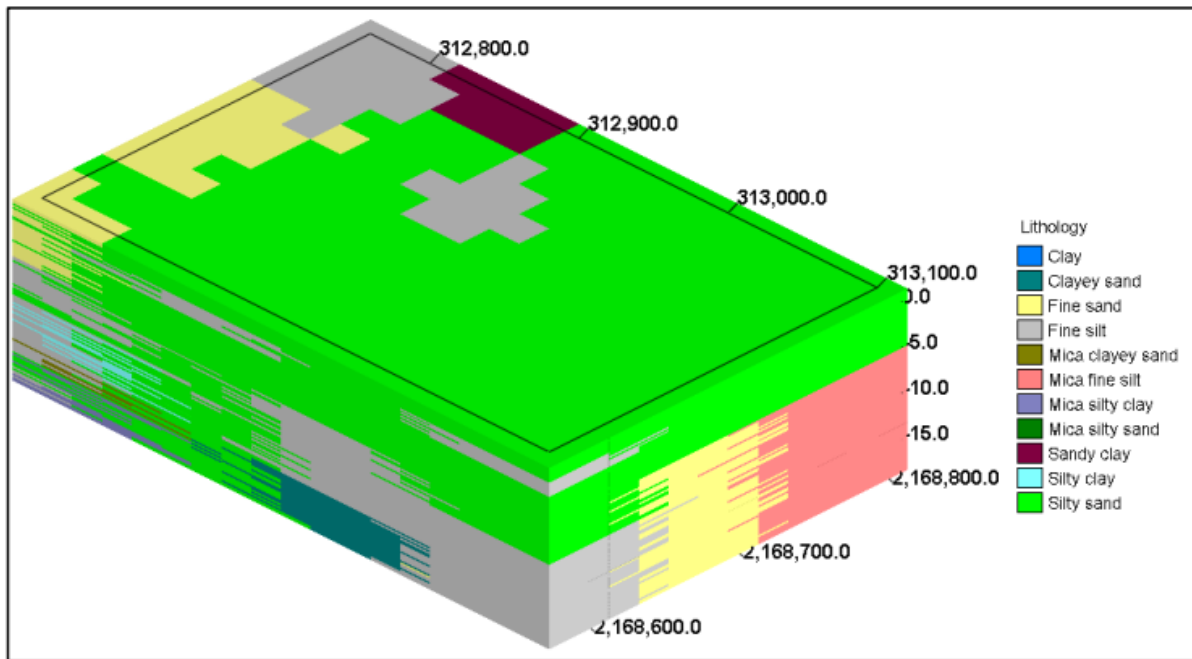
Various soil types have been noticed in borehole logs, with a gradation of soil particle size. These particles are represented in fine sand, silt, and clay. The presence of mica, a potentially problematic mineral in geotechnical engineering due to its impact on shear strength, was observed in certain soil horizons. The interpolation of borehole log data did not show the continuation of the layering of the soil properly (Figure 7). This phenomenon has been interpreted as the instability of Khor Mojj flow, controlled by the duration and intensity of rainfall in the highland of the Red Sea hills.

The loose to medium-dense soil layers comprise most of the research area. In the shallow surface, the SPT values in the northeast corner are comparatively lower than those on the opposite side, indicating greater soil stability in the southwest, per the SPT simulation results (Figure 8). The good news is that, as can be shown, the places with greater SPT values grow towards the deeper parts. This is bad news for geotechnical engineers involved in additional civil constructions in the district, particularly those who deal with shallow and deep foundations. At 15 meters below the surface, the safety factor rises to 1. The F.S. is precisely layered and depicted in various colours in Figure 9.

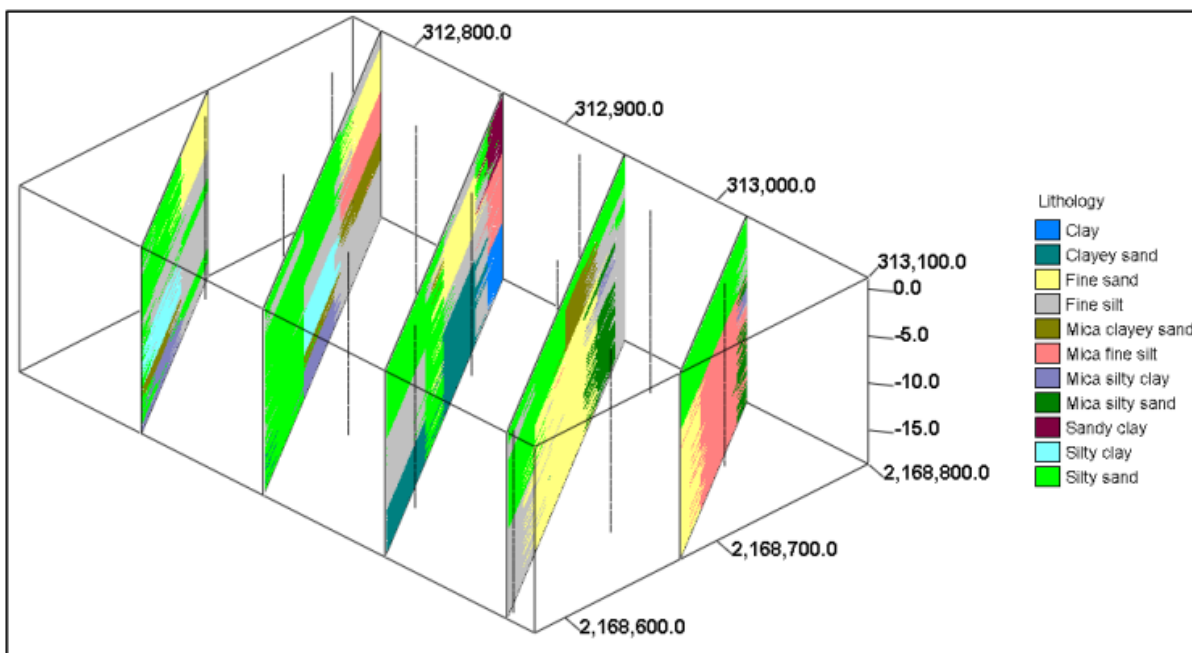
The constructed liquefaction potential model (Figure 10) shows that the liquefaction potential in the 7.5 earthquake scenario is moderate to high up to a depth of 15 m. The state is stable below this depth and does not liquefy under the same circumstances.

The safety factor and liquefaction potential index (LPI) simulations demonstrated the uniform layering of their properties, in contrast to the outcomes of lithology interpolation. This homogeneity is shown in Figs. 7, 8, and 10. The impact of overburden pressure on the strength characteristics of the soil has been cited as the reason for the homogeneity. Grain size has less of an effect on the soil cyclic resistance ratio than this effect does.

Due to the lack of seismic records in Port Sudan, the model results were cross-referenced with widely accepted LPI thresholds found in previous studies (e.g., [33], [34], [38–41], which is in line with our results in the present study.

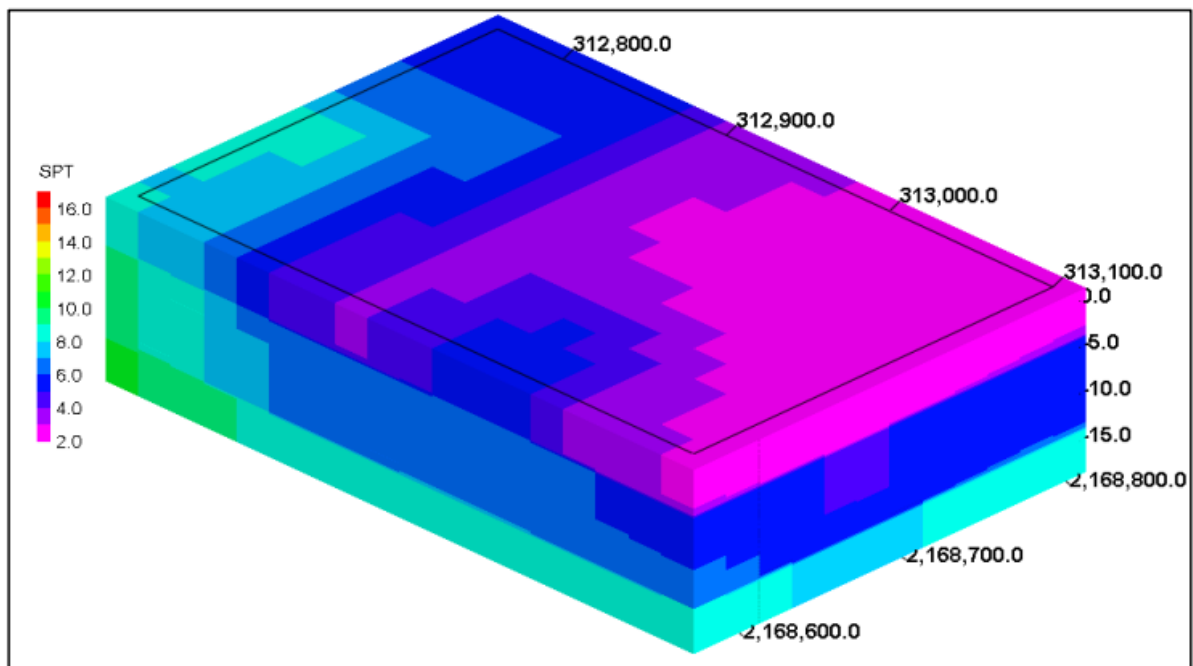


(a)

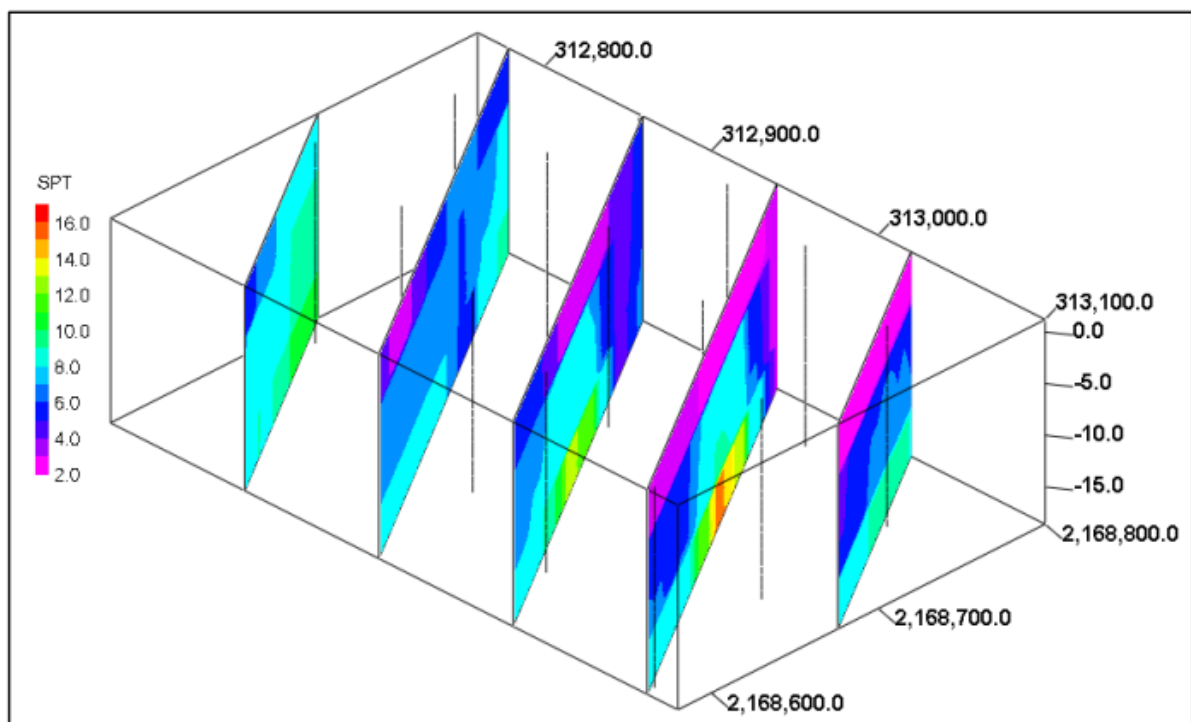


(b)

Figure 7. 3D modeling of the lithology of the study area; solid model (a), southeast–northwest cross sections (b), vertical exaggeration is 5 m

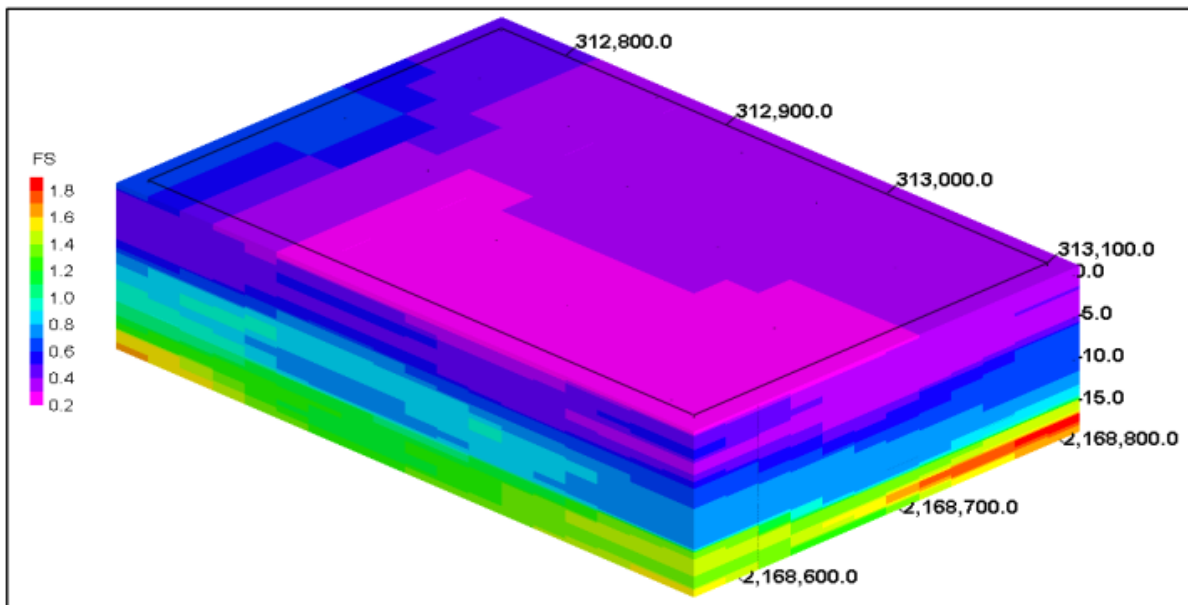


(a)

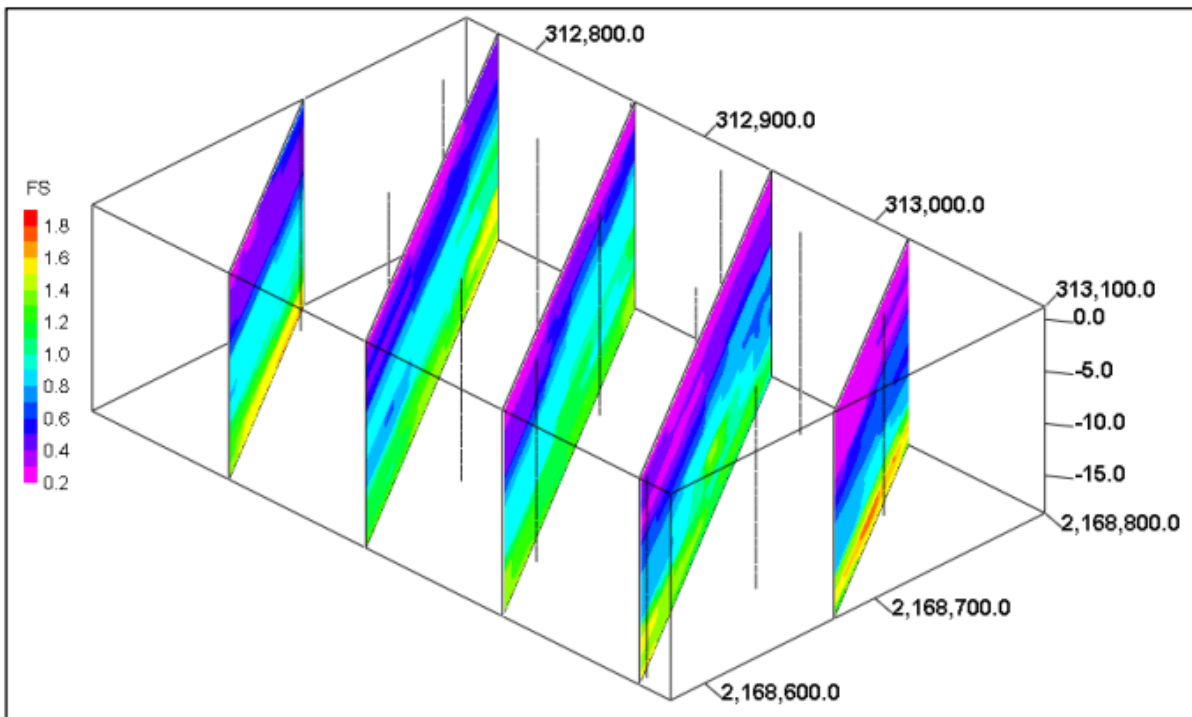


(b)

Figure 8. 3D modeling of the SPT Values of the study area; solid model (a), southeast–northwest cross sections (b), vertical exaggeration is 5 m

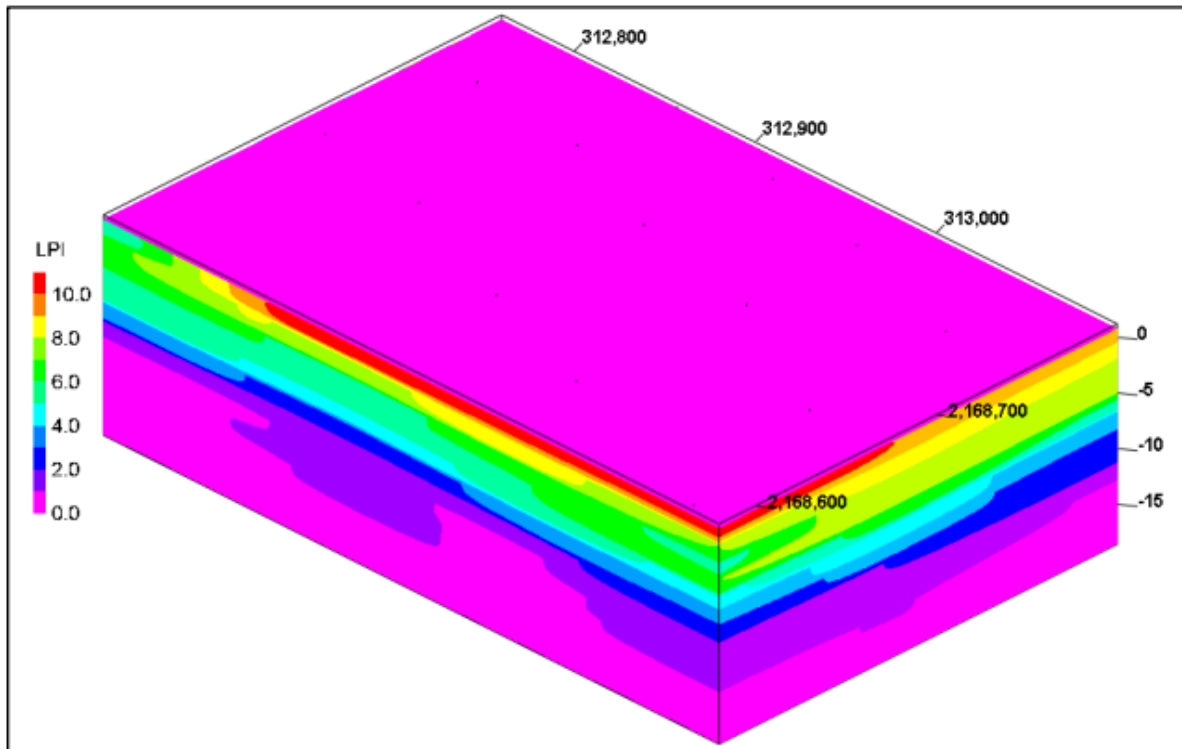


(a)

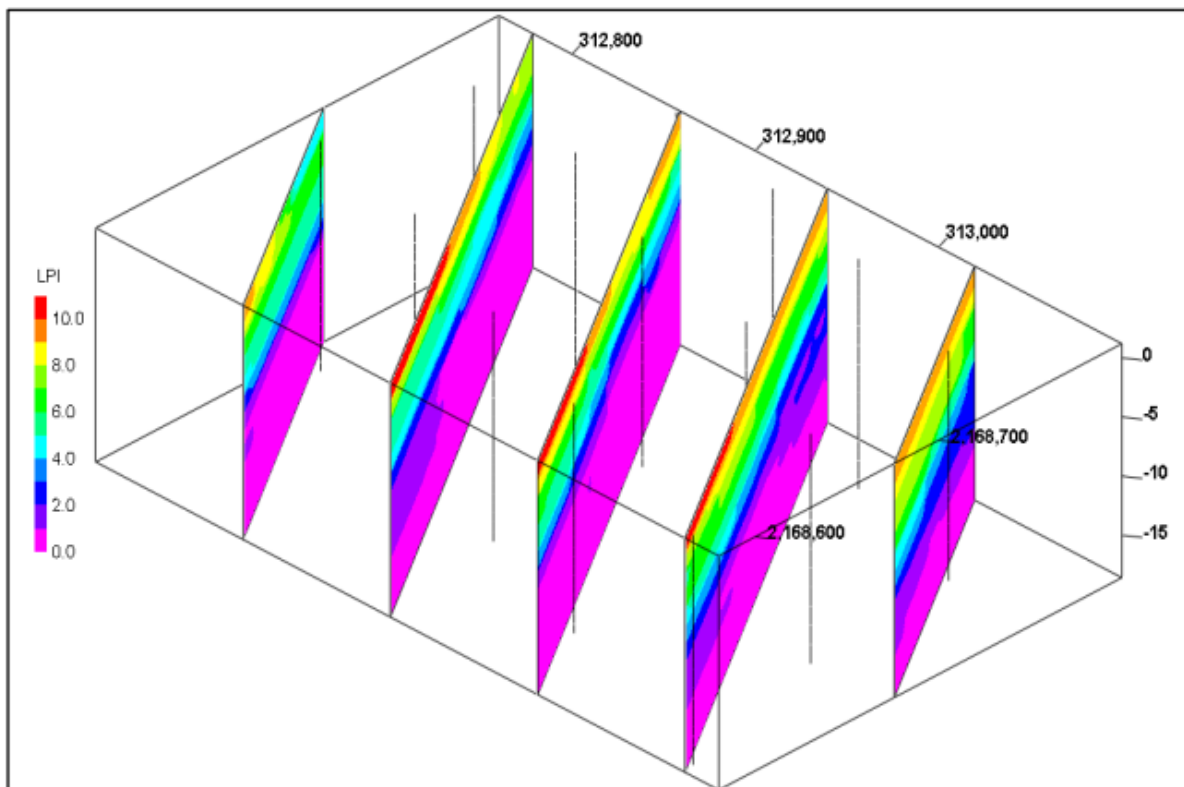


(b)

Figure 9. 3D modeling of the F.S. Values of the study area; solid model (a), southeast–northwest cross sections (b), vertical exaggeration is 5 m



(a)



(b)

Figure 10. 3D modeling of the LPI Values of the study area; solid model (a), southeast–northwest cross sections (b), vertical exaggeration is 5 m.

4. Conclusions

The SPT is widely utilised in many civil engineering projects to characterise the subsurface due to the simplicity of the equipment employed and the ease of the test procedure. The conclusion and remarks of the current study can be summed up as follows:

1. Saturated loose to medium-dense fine sand, silty sand, silt, and clay soil from the current natural ground surface down to roughly 25 meters deep make up most of the subsurface soil in the research region.
2. Subsurface water can be found between 0.9 and 1.9 meters below the surface.
3. The safety factor and thickness of the liquefiable layers have been used to estimate the liquefaction potential index (LPI). The values of each liquefaction potential index show that the soil horizons down to 15 meters are at very high risk of liquefaction from an earthquake of modest magnitude (about 7.5 Mw). The cyclic resistance ratio (CRR) and the cyclic stress ratio (CSR) have low values. As a result, the upper 15 meters of subsurface soil will be liquefied for a predetermined amount of time since the factor of safety (F.S.) is primarily smaller than one.
4. According to this study, an earthquake of magnitude 7.5 (Mw) will cause the saturated, loose, sandy, and silty soils of the alluvial valley-fill deposits at Port Sudan to liquefy. Therefore, these surface geological units must improve their ground before building structures.

4.1 Significance of the Work

This paper's findings on the liquefaction resistance of soils can be applied to enhance the ground condition in the Port Sudan region, paving the way for future urban development and the construction of earthquake-resistant buildings.

Acknowledgment

We want to thank the Sea Ports Corporation of Port Sudan for providing data and China University of Geosciences (Wuhan) for making the working environment available.

REFERENCES

- [1] Seed, H.B. and Idriss, I.M., 1971, Simplified procedure for evaluating soil liquefaction potential. *Journal of Soil Mechanics & Foundations Div.* <https://doi.org/10.1061/JSFEAQ.0001662>
- [2] Seed B.H., Tokimatsu, K., Harder, L.F., and Chung, R.M., 1985, Influence of SPT procedures in soil liquefaction resistance evaluations. *Journal of Geotechnical Engineering*, 1425–1445. [https://doi.org/10.1061/\(ASCE\)0733-9410\(1985\)111:12\(1425\)](https://doi.org/10.1061/(ASCE)0733-9410(1985)111:12(1425))
- [3] Youd, T.L., and Idriss, I.M., 2001, Liquefaction resistance of soils: summary report from the 1996 NCEER and 1998 NCEER/NSF workshops on evaluation of liquefaction resistance of soils. *Journal of geotechnical and geoenvironmental engineering*, 297–313. [https://doi.org/10.1061/\(ASCE\)1090-0241\(2001\)127:4\(297\)](https://doi.org/10.1061/(ASCE)1090-0241(2001)127:4(297))
- [4] Jha, S.K. and Suzuki, K., 2009, Reliability analysis of soil liquefaction based on standard penetration test. *Computers and Geotechnics*, 589–596. <https://doi.org/10.1016/j.compgeo.2008.10.004>
- [5] Juang, C.H., Ching, J., Luo, Z., and Ku, C.S., 2012. New models for probability of liquefaction using standard penetration tests based on an updated database of case histories. *Engineering geology*, 85–93. <https://doi.org/10.1016/j.enggeo.2012.02.015>
- [6] Sivrikaya, O. and Toğrol, E., 2006, Determination of undrained strength of fine-grained soils by means of SPT and its application in Turkey. *Engineering geology*, 52–69. <https://doi.org/10.1016/j.enggeo.2006.05.002>
- [7] Nasseh, S., Moghaddas, N.H., Ghafoori, M., Asghari, O., and Bazaz, J.B., 2018, Investigation of spatial variability of SPT data in Mashhad City (NE Iran) using a geostatistical approach. *Bulletin of Engineering Geology and the Environment*, 441–455. <https://doi.org/10.1007/s10064-017-1136-y>
- [8] Price, D.G., 2008, *Engineering geology: principles and practice*. Springer Science & Business Media. [Engineering Geology: Principles and Practice - David George Price - Google Books](https://books.google.com/books?id=UgEgEAAQAAQJ)
- [9] Shibata, T., & Teparaksa, W. (1988). Evaluation of liquefaction potentials of soils using cone penetration tests. *Soils and foundations*, 28(2), 49-60. https://doi.org/10.3208/sandf1972.28.2_49

- [10] Bray, J.D., Sancio, R.B., Travasarou, T., Durgunoglu, T., Onalp, A., Youd L.T. and Baturay, M.B., 2006, Closure to Subsurface Characterization at Ground Failure Sites in Adapazari, Turkey by Jonathan D. Bray, Rodolfo B. Sancio, Turan Durgunoglu, Akin Onalp, T. Leslie Youd, Jonathan P. Stewart, Raymond B. Seed, Onder K. Cetin, Ertan Bol, MB Baturay, C. Christensen, and T. Karadayilar. *Journal of Geotechnical and Geoenvironmental Engineering*, 541–547. [https://doi.org/10.1061/\(ASCE\)1090-0241\(2006\)132:4\(541\)](https://doi.org/10.1061/(ASCE)1090-0241(2006)132:4(541))
- [11] Boulanger, R.W. and Idriss, I.M., 2012, Probabilistic standard penetration test–based liquefaction–triggering procedure. *Journal of Geotechnical and Geoenvironmental Engineering*, 1185–1195. [https://doi.org/10.1061/\(ASCE\)GT.1943-5606.0000700](https://doi.org/10.1061/(ASCE)GT.1943-5606.0000700)
- [12] Zhang, G., Robertson, P.K., and Brachman, R.W.I., 2004, Estimating liquefaction-induced lateral displacements using the standard penetration test or cone penetration test. *Journal of Geotechnical and Geoenvironmental Engineering*, 861–871. [https://doi.org/10.1061/\(ASCE\)1090-0241\(2004\)130:8\(861\)](https://doi.org/10.1061/(ASCE)1090-0241(2004)130:8(861))
- [13] Idriss, I.M. and Boulanger, R.W., 2010, CPT, and SPT based liquefaction triggering procedures. Report No. UCD/CGM, 10, 2, 4–13. [Idriss Boulanger SPT Liquefaction CGM-10-02-with-cover-page-v2.pdf \(dlwqtxtslxzle7.cloudfront.net\)](https://doi.org/10.1061/(ASCE)GT.1943-5606.0000700)
- [14] Johnson, P.R., and Woldehaimanot, B., 2003, Development of the Arabian-Nubian Shield: perspectives on accretion and deformation in the northern East African Orogen and the assembly of Gondwana. Geological Society, London, Special Publications, 289–325. <https://doi.org/10.1144/GSL.SP.2003.206.01.15>
- [15] Wadi, D., Wu, W., Fuad, A., Ahmed, H. E., & Abdalla, R. (2022). Correlation between SPT and CPT for Sandy Soils in Port Sudan City using the Linear Regression Model. *African Journal of Engineering & Technology*. 6 (2022) 2 <https://doi.org/10.47959/AJET.2021.1.1.6>
- [16] Ross, D.A. and Schlee, J., 1973, Shallow structure and geologic development of the southern Red Sea. *Geological Society of America Bulletin*, 3827–3848. [https://doi.org/10.1130/0016-7606\(1973\)84<3827:SSAGDO>2.0.CO;2](https://doi.org/10.1130/0016-7606(1973)84<3827:SSAGDO>2.0.CO;2)
- [17] McKenzie, D., 1978, Some remarks on the development of sedimentary basins. *Earth and Planetary science letters*, 25–32. [https://doi.org/10.1016/0012-821X\(78\)90071-7](https://doi.org/10.1016/0012-821X(78)90071-7)
- [18] Foster, A.N. and Jackson, J.A., 1998, Source parameters of large African earthquakes: implications for crustal rheology and regional kinematics. *Geophysical Journal International*, 422–448. <https://doi.org/10.1046/j.1365-246x.1998.00568.x>
- [19] Wernicke, B., 1985, Uniform-sense normal simple shear of the continental lithosphere. *Canadian Journal of Earth Sciences*, 108–125. <https://doi.org/10.1139/e85-009>
- [20] Voggenreiter, W., Hötzl, H., and Jado, A.R., 1988, Red Sea related history of extension and magmatism in the Jizan area (Southwest Saudi Arabia): indication for simple-shear during early Red Sea rifting. *Geologische Rundschau*, 257–274. <https://doi.org/10.1007/BF01848688>
- [21] McGuire, A.V. and Bohannon, R.G., 1989, Timing of mantle upwelling: Evidence for a passive origin for the Red Sea Rift. *Journal of Geophysical Research: Solid Earth*, 1677–1682. <https://doi.org/10.1029/JB094iB02p01677>
- [22] Camp, V.E. and Roobol, M.J., 1992, Upwelling asthenosphere beneath western Arabia and its regional implications. *Journal of Geophysical Research: Solid Earth*, 15255–15271. <https://doi.org/10.1029/92JB00943>
- [23] Bellahsen, N., Faccenna, C., Funicello, F., Daniel, J.M., and Jolivet, L., 2003, Why did Arabia separate from Africa? Insights from 3-D laboratory experiments. *Earth and Planetary Science Letters*, 365–381. [https://doi.org/10.1016/S0012-821X\(03\)00516-8](https://doi.org/10.1016/S0012-821X(03)00516-8)
- [24] Abril, J.M. and Perriñez, R., 2017, A modelling study on tsunami propagation in the Red Sea: Historical events, potential hazards and spectral analysis. *Ocean Engineering*, 1–12. <https://doi.org/10.1016/j.oceaneng.2017.02.008>
- [25] ASTM D6066, 1996, Standard practice for determination of the normalized penetration resistance of sands for evaluation of liquefaction potential. In *Annual Book of ASTM Standards*, American Society of Testing Material.
- [26] ASTM D1586, 1999, Standard Method for Penetration Test & Split-Barrel Sampling of Soils, *Annual Book of Stds*, 4.08. ASTM, Philadelphia, 139–143.
- [27] Iwasaki, T., Tokida, K.I., Tatsuoka, F., Watanabe, S., Yasuda, S., and Sato, H., 1982, June, Microzonation for soil liquefaction potential using simplified methods. In *Proceedings of the 3rd international conference on microzonation*, Seattle, pp. 1310–1330.
- [28] Skempton, A., 1986, Standard penetration test procedures and the effects in sands of overburden pressure, relative density, particle size, ageing and overconsolidation. *Geotechnique*, 425–447. <https://doi.org/10.1680/geot.1986.36.3.425>
- [29] Seed, H.B. and Idriss, I.M., 1967, Analysis of soil liquefaction: Niigata earthquake. *Journal of the Soil Mechanics and Foundations Division*, 83–108. <https://doi.org/10.1061/JSFEAQ.0000981>
- [30] Esteva, L. (1987). Earthquake engineering research and practice in Mexico after the 1985 earthquakes. *Bulletin of the New Zealand Society for Earthquake Engineering*, 20(3), 159-200.

- [31] Cetin, K.O., Seed, R.B., Der Kiureghian A, Tokimatsu K, Harder L.F., Kayen R.E., and Moss R.E., 2004. Standard penetration test-based probabilistic and deterministic assessment of seismic soil liquefaction potential. *Journal of geotechnical and geoenvironmental engineering*, 1314–1340. [https://doi.org/10.1061/\(ASCE\)1090-0241\(2004\)130:12\(1314\)](https://doi.org/10.1061/(ASCE)1090-0241(2004)130:12(1314))
- [32] Idriss, I.M. and Boulanger, R.W., 2006, Semi-empirical procedures for evaluating liquefaction potential during earthquakes. *Soil Dynamics and Earthquake Engineering*, 115–130. <https://doi.org/10.1016/j.soildyn.2004.11.023>
- [33] Sonmez, H. and Gokceoglu, C., 2005, A liquefaction severity index suggested for engineering practice. *Environmental Geology*, 81–91.
- [34] Sonmez, H., 2003, Modification of the liquefaction potential index and liquefaction susceptibility mapping for a liquefaction-prone area (Inegol, Turkey). *Environmental Geology*, 862–871.
- [35] Wadi, D., Wu, W., Malik, I., Ahmed, H. A., and Makki, A. (2021). Assessment of liquefaction potential of soil based on standard penetration test for the upper Benue region in Nigeria. *Environmental Earth Sciences*, 1–11. <https://doi.org/10.1007/s12665-021-09565-y>
- [36] Matheron, G., 1963, Principles of geostatistics. *Economic geology*, 1246–1266. <https://doi.org/10.2113/gsecongeo.58.8.1246>
- [37] Leuangthong, O., McLennan, J.A., and Deutsch, C.V., 2004, Minimum acceptance criteria for geostatistical realizations. *Natural Resources Research*, 131–141. <https://doi.org/10.1023/B:NARR.0000046916.91703.bb>
- [38] Delbari, M., Afrasiab, P., and Loiskandl, W., 2009, Using sequential Gaussian simulation to assess the field-scale spatial uncertainty of soil water content. *Catena*, 163–169. <https://doi.org/10.1016/j.catena.2009.08.001>
- [39] Iwasaki, T., Arakawa, T., and Tokida, K.I., 1984, Simplified procedures for assessing soil liquefaction during earthquakes. *International Journal of Soil Dynamics and Earthquake Engineering*, 49–58. [https://doi.org/10.1016/0261-7277\(84\)90027-5](https://doi.org/10.1016/0261-7277(84)90027-5)
- [40] Kayen, R. E., Mitchell, J. K., Seed, R. B., Lodge, A., Nishio, S. Y., & Coutinho, R. (1992, May). Evaluation of SPT-, CPT-, and shear wave-based methods for liquefaction potential assessment using Loma Prieta data. In *Proc., 4th Japan-US Workshop on Earthquake-Resistant Des. of Lifeline Fac. and Countermeasures for Soil Liquefaction (Vol. 1, pp. 177-204)*.
- [41] Holzer, T.L., Noce, T.E., Bennett, M.J., Tinsley III, J.C., and Rosenberg, L.I., 2005, Liquefaction at Oceano, California, during the 2003 San Simeon earthquake. *Bulletin of the Seismological Society of America*, 2396–2411. <https://doi.org/10.1785/0120050078>